Food Research International 160 (2022) 111621

Contents lists available at ScienceDirect

Food Research International

journal homepage: www.elsevier.com/locate/foodres

A unifying approach to lipid oxidation in emulsions: Modelling and experimental validation

Karin Schroën[a,b,*], Claire C. Berton-Carabin[a,c]

[a] Wageningen University, Department of Agrotechnology & Food Sciences, Laboratory of Food Process Engineering Group, Bornse Weilanden 9, 6708 WG Wageningen, the Netherlands
[b] Membrane Processes for Food Group, University of Twente, Drienerlolaan 5, 7522 NB Enschede, the Netherlands
[c] INRAE, UR BIA, F-44316 Nantes, France

A R T I C L E I N F O

Keywords:
Lipid oxidation
Emulsion
Modelling reaction kinetics
Emulsifier
Food

A B S T R A C T

Lipid oxidation is a longstanding topic within the field of food technology, and is strongly related to loss of product quality and consumer acceptance. Both for bulk oils and emulsions, the chemical phenomena involved in lipid oxidation have been extensively researched, and various reaction pathways have been identified. They are different in bulk oil compared to oil-in-water (O/W) emulsions in which the oil–water interface plays a prominent role. Most probably because of the complexity of the reaction scheme in combination with mass transfer effects, there is no model that describes lipid oxidation in emulsions in a unified fashion, and that is the aim that we have set ourselves to achieve.

We use lipid oxidation data previously obtained in O/W emulsions made with 5 different emulsifiers (2 surfactants, and 3 proteins), in well-mixed systems where the oxygen-to-oxidizable lipid ratio is strictly controlled. We use data pertaining to headspace oxygen concentration, and to primary and secondary lipid oxidation products to develop a model based on reaction kinetics, including not only the classical reaction scheme (starting from an unsaturated lipid, LH) but also radical initiation from hydroperoxides, which is thought to be an effect that is overlooked in the classical description of the initiation step.

We were able to describe the course of the reactions in these emulsions using the same reaction rate constants for all emulsions, with the exception of the two related to radical-based initiation. In Tween 20- and Tween 80-stabilized emulsions, initiation stems most probably solely from decomposition of hydroperoxides; this implies that lipid oxidation in these emulsions is co-determined by the initial ("pre-existing") hydroperoxide concentration. In protein-stabilized emulsions, on the other hand, lipid radical initiation is probably linked to reactions involving proteins (co-oxidation reactions), whereas initiation through decomposition of hydroperoxides seems less important, if at all. From this, we can conclude that the difference between both types of emulsions with regard to lipid oxidation mechanisms is related to differences in radical initiation.

The developed model can serve as a unified basis for understanding lipid oxidation in emulsions, through which additional effects beyond the bare reaction kinetics, such as mass transfer effects, can be identified and used to e.g., quantify antioxidant effects, which is part of follow-up research.

1. Introduction

In nature, various complex chemical reactions take place, in which not only reaction kinetics plays a role, but also compartmentalization of components in combination with various mass transfer effects. An illustrative example are living cells, in which a large number of cascaded reactions can take place, and that are controlled through the localization of e.g., enzymes, transport through pumps that regulate ionic species, and compartmentalization by the cell membrane that generally keeps external influences to a minimum. Besides, cells and micro-organisms can be encouraged to produce a range of components during fermentations, of which the products and their concentrations can be steered by smart feeding and mixing strategies (Riet & Tramper, 1991). In order to manage these reactions, modelling is a trusted tool that reduces

---

* Corresponding author at: Wageningen University, Department of Agrotechnology & Food Sciences, Laboratory of Food Process Engineering Group, Bornse Weilanden 9, 6708 WG Wageningen, the Netherlands.

E-mail addresses: karin.schroen@wur.nl (K. Schroën), claire.berton-carabin@inrae.fr (C.C. Berton-Carabin).

https://doi.org/10.1016/j.foodres.2022.111621
Received 22 March 2022; Received in revised form 11 June 2022; Accepted 1 July 2022

experimental work considerably once the underlying kinetics are understood (which is far from trivial; see e.g., Westerterp, Van Swaaij, & Beenackers, 1987).

In food production, various cascaded reactions are of great relevance. A well-known example would be the Maillard reaction, which can lead to desirable as well as undesirable food properties (Lund & Ray, 2017), and of which still not all details have been unraveled, even though various modelling approaches have been used to capture reaction kinetics (Boekel, 2001; Martins, Jongen, & Boekel, 2001). Lipid oxidation is also one of these illustrative reactions that has kept many researchers occupied over the years, and is still a very active field of research. Both reviews on oxidation in bulk oil (Conte et al., 2020; Manzocco, Calligaris, Anese, & Nicoli, 2016), and in emulsions (which is related to shelf-life) have been published (Coupland & Mcclements, 1996; Laguerre, Tenon, Bily, & Birti, 2020; McClements & Decker, 2000).

In general, bulk oil oxidizes slower than emulsified oil (Ghnimi, Budilarto, & Kamal-Eldin, 2017), which has been related to effects taking place at the interface (e.g., iron-based initiation of oxidation, attraction of metal cations to the interface by negatively charged emulsifiers, other pro-oxidant effects created by emulsifiers such as oxidizing proteins, and so on; (Chung & McClements, 2014; Johnson & Decker, 2015; Chaprenet et al., 2014; Berton-Carabin, Ropers, Guibert, Solé, & Genot, 2014). Furthermore, it has been suggested that mass transfer of reactants within the emulsion plays an important role in propagating lipid oxidation (Mickael Laguerre, Bily, Roller, & Birti, 2017), e.g., by transfer of hydroperoxides in micelles (Coupland & Mcclements, 1996; Erramreddy, Tu, & Ghosh, 2017; Miyashita, 2014), or through concentration gradients under non-ideally mixed circumstances.

In literature, a plethora of effects have been proposed to explain how lipid oxidation occurs in emulsions, and why differences are observed between various formulations. The big question that we are trying to help answering is not so much whether something occurs, but at which rate and to which extent; so, whether it is relevant for the general overall behavior of the reacting system. In literature, some approaches have been suggested, such as using initial reaction rates (Manzocco et al., 2016), or linearized parts of a curve (Conte et al., 2020). In doing so, the fact that a cascade of reactions is at work, leading to continuous changes in concentrations that thus also influence other reactions is overlooked. Furthermore, whether these changes are a result of either the reaction kinetics or mass transfer effects remains elusive since this is in general not mentioned, nor considered.

The situation is actually similar to that encountered in large reactor systems used for chemicals production. Also there, reaction kinetics in combination with mass transfer leads to an overall effect that can cause a lot of confusion. In order to defuse this situation, first, various aspects need to be investigated under controlled conditions that favor specific effects that are related to the reaction. Although this is a standard procedure in chemical engineering, in lipid oxidation research this is not the case. This is understandable, because some reaction components are transient and/or difficult to measure (such as the radicals).

It is good to mention that various attempts have been made to take information from the obtained lipid oxidation curves using mathematical equations that resemble the shape (growth curves based on Gompertz, logistic, of Weibull models (Pinchuk & Lichtenberg, 2014)), which leads to more in-depth understanding of system behavior and allows for comparisons between formulations on an objective basis (e.g., Merkx, Swager, van Velzen, van Duynhoven, & Hennebelle, 2021; Berton-Carabin, Ropers, Guibert, Solé, & Genot, 2014; Farhoosh, 2020). The first two references consider emulsions, and the last one focusses on bulk oil. Also dapper attempts have been made to cover effects taking place at the interface using e.g., pseudophase models that were applied to emulsions (Bravo-Díaz, 2022; Romsted & Bravo-díaz, 2013). In the current paper, we want to go beyond this, and create a unifying approach to describe lipid oxidation in emulsions in a quantitative way, starting from basic reaction kinetics, and reactor design considerations. In doing so, we go far beyond how lipid oxidation is currently approached, i.e., pinpointing differences in oxidation products at points in time that are taken 'at random', without considering the reaction system as a whole (so the intrinsic reaction and mass transfer conditions).

Our ultimate goal is to develop an approach, and through that a model that can be used to describe lipid oxidation in food emulsion products that have a relatively high content in omega-3 polyunsaturated fatty acids (PUFAs) and that are thus prone to oxidation, albeit very much preferred from a health point of view (Calder, 2021). In order to distinguish between effects related to reaction kinetics and mass transfer, we have worked on an extensive series of experimental data, previously published (Berton, Genot, Viau, & Genot, 2011) in which very specific reaction conditions were used (continuous mixing, low emulsion-to-headspace ratio, and relatively low concentrations of emulsifiers – such that non-adsorbed emulsifier concentrations were minimized). The components that were analyzed allow us to investigate various stages of oxidation (oxygen consumption, primary oxidation products, and volatile secondary oxidation products, propanal and hexanal), as extensively discussed in standard works such as those of Schaich (e.g., (Schaich, 2005). In the materials and methods section, more details on the approach that we used, and the selection of reaction conditions are given. Although secondary oxidation products are covered, our work excludes sensory effects and modelling thereof; for that we refer through to the work of the group of Charlotte Jacobsen (Jacobsen, 1999; Venkateshwarlu, Let, Meyer, & Jacobsen, 2004).

As emulsifiers, we consider three proteins (β-lactoglobulin, bovine serum albumin, sodium caseinate) and two surfactants (Tween 20 and Tween 80). The basic equations that we use to describe the reaction kinetics are very classic (Coupland & Mcclements, 1996; Laguerre et al., 2017), with the exception of the last one that has been proposed in the latter reference, and becomes more and more substantiated as we speak.

$LH \rightarrow L^{\cdot} + H$	(1) Alkyl radical formation.
$L^{\cdot} + O_2 \rightarrow LOO^{\cdot}$	(2) Oxygen addition to form peroxyl radicals.
$LOO^{\cdot} + LH^{'} \rightarrow LOOH$	(3) Propagation: Formation of hydroperoxides (primary oxidation products).
$LOOH \rightarrow LO^{\cdot} \rightarrow \text{non-radical products}$	(4) Hydroperoxide decomposition to form alkoxyl radicals, and in turn secondary oxidation products.
$LOOH \rightarrow LOO^{\cdot}$	(5) Hydroperoxide decomposition to peroxyl radicals.

The reactions used in the present work, and their interconnections are shown in Fig. 1. When starting from a non-oxidized fatty acid LH, an alkyl radical $L^{\cdot}$ (reaction (1)) is formed, that subsequently reacts with O_2 to form a peroxyl radical $LOO^{\cdot}$ (reaction (2)), that in turn can react with another non-oxidized fatty acid LH' (reaction 3) to form a hydroperoxide (LOOH, primary oxidation product; reaction 3), that then can react either through to a secondary product LO via a number of steps that we here simply to one (reaction 4), or generate a new radical (reaction 5). To be complete, reaction 5 is initiated by Fe^{3+} leading to Fe^{2+} and $LOO^{\cdot}$; Fe^{2+} is converted back to Fe^{3+} by reaction with LOOH giving $LO^{\cdot}$, that leads to LOH. Since we did not measure LOH components, and they have been reported as minor (~0.2–0.3 %, see discussion reaction rate constants), the reaction to LOH was not incorporated in the model.

In the model, we cover conjugated diene hydroperoxides and other hydroperoxides; both originating from polyunsaturated fatty acids (PUFAs). Since monounsaturated acids (MUFAs) are known to have reactivity that is much lower (at least 30-fold up to 50-fold or even more (Holman & Elmer, 1947; Pratt, Mills, & Porter, 2003)), we did not consider them separately in the reaction scheme. This choice is further supported by the fact that no decrease in MUFA concentration could be experimentally detected in the β-lactoglobulin-stabilised emulsion that oxidized most rapidly of all emulsions considered here (Berton, Ropers, Guibert, Solé, & Genot, 2012). The reaction rate constants for the

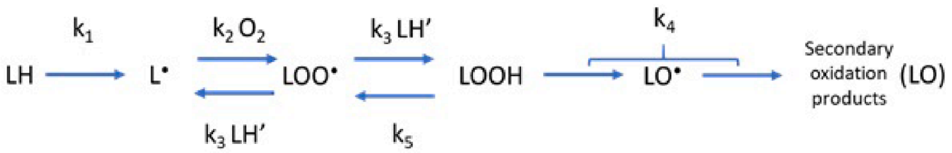

Fig. 1. Overview of reactions incorporated in the model: LH/LH' is unreacted fatty acid, $L^{\bullet}$ radical, $LOO^{\bullet}$ oxidized radical, LOOH primary oxidation product (conjugated dienes were measured in our experiments), $LO^{\bullet}$ secondary oxidation products (hexanal and propanal were measured), and O_2 oxygen which was also measured.

formation of conjugated dienes and other hydroperoxides were initially taken equal, and later adjusted (slightly) to improve the description of the reactions found (see model development section).

It is good to point out that termination reactions via radical recombination are not considered in the model, for that we refer to literature (Farhoosh, 2020). As mentioned earlier, we will use reactions (1)–(5) to analyse results that were previously published (Berton, Genot, Viau, & Genot, 2011), and that were obtained under very well defined conditions (see definition of reaction system section). It is good to mention that the choice of the reaction conditions was instrumental for reaching the unification that we strive for; mass transfer greatly exceeds reaction rates, making the emulsions behave as if 'ideally mixed' on droplet level.

We are indeed able to apply our approach to all emulsions studied, and find great resemblance in the values of the reaction rate constants, with as exception those related to radical formation (reactions 1 and 5). We expect that effects taking place near the interface are responsible for this. In the outlook section we elaborate on model sensitivity, and the effects that various measuring methods may have on oxidation in emulsions.

2. Materials and methods

2.1. Materials

Although the experimental results were published earlier (Berton, Genot, Viau, et al., 2011), we have chosen to reproduce part of the materials and methods section here for reader convenience, focusing on the chosen oil, surfactants, and oxidation analysis.

Rapeseed oil was purchased in a local supermarket. It was stripped by means of alumina (MP Alumina *N*-Super I, MP Biomedicals, France) to eliminate impurities and tocopherols (less than 2 μg residual tocopherols per g oil). Bovine serum albumin (BSA) (minimum 96 % by agarose gel electrophoresis) was obtained from MP Biomedicals (France). β-Casein (BCN) (purity ≥ 98 %) was purchased from Lactalis (France). β-Lactoglobulin (BLG) was purified from whey protein isolate (Prolacta 90, Lactalis, France) by selective precipitation. Tween 20, Tween 80, 1,4-piperazinediethanesulfonic acid (PIPES), ethylene diamine tetra-acetic acid disodium calcium salt (EDTA) and iron (II) sulfate ($FeSO_4$) were purchased from Sigma Aldrich (France). The neutral buffer was composed of PIPES (10 mM) and NaCl (80 mM) and adjusted to pH 6.7.

2.2. Emulsions and lipid oxidation measurements

2.2.1. Preparation and physical characterization of O/W emulsions

The day before emulsion preparation, the emulsifiers (proteins or surfactants) were dispersed in buffer (pH 6.7) and gently stirred overnight at 4 °C to ensure their complete solubilization without foam formation.

O/W emulsions were prepared with 30 g oil and 70 g aqueous solution per 100 g of emulsion. The two phases were premixed for 2 min at 15000 rpm using a rotor–stator homogenizer fitted with a 12-mm diameter head (Polytron PT 3000, Kinematica, Littau, Switzerland). The coarse emulsions were then homogenized through a one-stage low-pressure valve homogenizer (A0812W-A-CD, Stansted Fluid Power, Stansted, UK). The size distribution of oil droplets in the emulsions was measured immediately after homogenization with a laser light scattering instrument (Saturn 5200, Micromeritics, Verneuil en Halatte, France). The emulsifier concentration, pressure, and time of emulsification were adjusted to produce stable emulsions with concentrations of unadsorbed emulsifiers as low as possible but a similar narrow droplet size distribution and average droplet size ([d3,2] initially between 1.4 and 1.8 μm: see table 2). Concentrations of emulsifiers in aqueous solutions were 4 g/L for BSA and 5 g/L for BCN, BLG, Tween 20, and Tween 80. Protein-stabilized emulsions were homogenized for 10 min at 50 bar, and surfactant-stabilized emulsions were homogenized for 5 min at 35 bar.

For each emulsifier, at least two emulsions were prepared independently. Oxygen uptake was measured in two vials, with three headspace samplings per vial; conjugated dienes (CD) were measured in one vial, with three samplings per vial; volatile compounds were analyzed in one vial, with one sampling per vial.

2.2.2. Incubation of emulsions

The emulsions were incubated in the presence of an oxidation initiator made of an equimolar mixture of $FeSO_4$ and EDTA (1/1, M/M, final concentration in emulsions 200 μM). Aliquots (3 mL) of emulsions were distributed in 20.5-mL headspace vials and hermetically sealed. Incubation was held at 25 °C, and all the detailed conditions are described in (Berton, Genot, Viau, et al., 2011).

2.2.3. Measurements of lipid oxidation

2.2.3.1. Oxygen uptake. Oxygen uptake was determined by taking a sample (100 μL) of headspace that was injected with a gas-tight syringe and gas chromatography (GC) analysis was performed with a HP 5890 series II gas chromatograph (Hewlett-Packard, Böblingen, Germany) coupled to a thermal conductivity detector (TCD) in isothermal mode at 50 °C, and helium as carrier gas. Peaks corresponding to oxygen were integrated and normalized to the peak area of ambient air. The amount of residual oxygen in the headspace of the vials was calculated from the theoretical proportion of oxygen in air and the volume of headspace in the vials. Results were expressed in mmol of oxygen per kg of oil (mmol O_2 kg^{-1} oil).

There is a peculiarity in this measurement that is good to point out, and that we also noted in many other experiments. In the originally published results (Berton, Genot, Viau, et al., 2011), late in the reaction, the measured oxygen concentrations seem to level of at a non-zero value, and sometimes even seem to increase. This is not possible in a system in which oxygen is the limiting substrate, as we will explain later. We expect that this is caused by the fact that the headspace of the vials has an under pressure due to approximately 1/5 of the amounts of molecules in the gas phase having reacted away (oxygen would be ∼ 21 % of the total in the starting air). As soon as the needle is removed from the incubation vessel, a small amount of air will be sucked in, leading to an increase in the oxygen present that at most corresponds to 8 mM oxygen/kg oil. This will influence the concentrations measured; therefore, we adjusted the oxygen concentrations accordingly, by increasing the oxygen consumption rate with 21 %, or phrased differently by increasing the difference between the initial oxygen concentration and the measured oxygen concentration by 21 %.

2.2.3.2. Conjugated diene (CD) hydroperoxides. The formation of CD hydroperoxides, which are primary oxidation products from PUFAs, was determined according to the method described by Lethuaut et al. (Lethuaut, Métro, & Genot, 2002). Aliquots of emulsions were diluted in isopropanol. The resulting solutions were centrifuged, and the absorbance of the supernatants was measured at 233 nm with a UV − visible spectrophotometer. Results were expressed in mmol of equivalent hydroperoxides per kg of oil (mmol eq HP kg^{-1} oil) using 27000 M^{-1} cm^{-1} as the molar extinction coefficient of CD at 233 nm.

2.2.3.3. Volatile compounds. The formation of secondary oxidation products was evaluated measuring two volatile compounds (propanal and hexanal) in the headspace of the samples. Briefly, these compounds were analyzed by GC paired with a flame ionization detector (FID) after their adsorption on a solid phase microextraction (SPME) fiber during exposure in the headspace of the vials for 15 min at 25 °C. The peak areas were converted into amounts of volatile compounds (μmol kg^{-1} oil) using external calibration curves (Berton, Genot, Viau, et al., 2011).

2.3. Definition and characterization of the reaction system

The various concentrations that are used are all based on kilograms of oil initially present. Rapeseed oil contains the following oxidizable fatty acids C18:1n-9, C18:2n-6 and C18:3n-3 at 618.5, 191.7, and 92.2 mg/g oil respectively (Berton, Genot, Viau, et al., 2011). The amount of oxygen that is present is calculated based on the gas composition of the headspace, and on the amount of oxygen dissolved in both water and oil at 25 °C (for the solubility of oxygen in water, the value of 8.5 mg/L is used (Karbowiak et al., 2010; engineering toolbox), whereas for oil this value is 45 mg/L (Cuvelier, Soto, Courtois, Broyart, & Bonazzi, 2017)). We chose to work with a surplus of oxidizable fatty acids compared to the total amount of oxygen present to prevent running into limitations early on in the reaction.

The average initial droplet size in the emulsions is between 1.4 and 1.8 μm, and the emulsions are incubated under gentle mixing. Whether this also leads to a system that is reaction-dominated, we deduce from dimensionless numbers to illustrate which behavior can be expected. We start with Damköhler II, that relates chemical reaction rate to diffusive mass transfer as follows:

$$\mathrm{DaII} = \frac{k_r \bullet d^2}{D} \tag{I}$$

With k_r the *first* order reaction rate constant (see model development section), *d* the characteristic dimension, which in our case is the droplet size (ranging from 1.4 to 1.8 μm), and *D* the diffusion coefficient of triglycerides that are the slowest lipid diffusing species ($5 \cdot 10^{-14}$ m^2/s; (Callaghan & Jolley, 1980)). When keeping the results that we obtain later in mind (k_r of $10^{-5} - 10^{-3} h^{-1}$), we find that the reaction is the rate-determining factor (Da II ranging from 10^{-7}-10^{-5}) if we consider mass transfer to be diffusion-based (as would be the case inside an oil droplet). Mass transfer in the continuous phase takes place under convective conditions and is expected to be much faster, therewith confirming that substrate (in the widest sense since many products are the substrates for other reactions) concentration gradients expectedly do not play a role in the emulsions that we investigated.

This conclusion was confirmed using Fick's law as a starting point for calculating concentration equilibration within a droplet.

$$J = D \bullet \frac{dC}{dx} \tag{II}$$

With *J*, the diffusion flux, *dC* the difference in concentration, and *dx* the difference in position of diffusing species.

Typical times needed for oxygen equilibration assuming a zero concentration at the beginning are ≪ 1 s, and for triglycerides in the order of a second. Therefore, we can assume ideally mixed conditions in the emulsion droplets, and emulsions.

In the outlook section we will use the same approach to illustrate effects that may take place in emulsions that are standing still, or that are opened for sampling, and resealed for further incubation.

2.4. Model development

The model focusses on reaction kinetics under ideally mixed conditions (see previous section for motivation thereof) and is based on standard equations that are first order in concentration. For the components of interest mentioned in the introduction (reactions (1)–(4)) the following ***rate equations*** are derived:

$\frac{d[L^{\cdot}]}{dt} = k_1 \bullet [LH] - k_2 \bullet [L^{\cdot}] \bullet [O_2]$	(III) $L^{\bullet}$ radical formation.
$\frac{d[LOO^{\cdot}]}{dt} = k_2 \bullet [L^{\cdot}] \bullet [O_2] - k_3 \bullet [LOO^{\cdot}] \bullet [LH^{'}] + k_5 \bullet [LOOH]$	(IV) $LOO^{\bullet}$ radical formation.
$\frac{d[LOOH]}{dt} = k_3 \bullet [LOO^{\cdot}] \bullet [LH^{'}] - k_4 \bullet [LOOH] - k_5 \bullet [LOOH]$	(V) Primary oxidation products.
$\frac{d[LO]}{dt} = k_4 \bullet [LOOH]$	(VI) Secondary oxidation products.

For propanal and hexanal formation, we use the same reaction as for the overall reaction for secondary oxidation products (equation VI), but use lower albeit constant *k*-values for all emulsions to do justice to the relative contribution of components to the overall concentration of secondary oxidation products. It is good to point out again, and also shown in Fig. 1, that k_4 is a lumped reaction rate, ultimately leading to formation of secondary oxidation products, which includes formation of $LO^{\bullet}$ radicals.

Furthermore, we use two ***mass balances*** to describe the entire reaction based on concentrations defined per kg oil in the emulsion. One mass balance describes oxygen and species that contain oxygen, whereas the other one keeps track of all oxidizable and oxidized species; in this way we track both substrates on mole basis as is customary in chemical engineering and biotechnology (e.g., Schroen et al., 2001).

$$[LH] + [L^{\cdot}] + [LOO^{\cdot}] + [LOOH] + [LO] = [LH]_{t=0} \tag{VII}$$

$$[O_2] + [LOO^{\cdot}] + [LOOH] + [LO] = [O_2]_{t=0} \tag{VIII}$$

In the experimental work, conjugated diene (CD) hydroperoxides were measured, that, by definition, stem from PUFAs (with at least 2 double bonds), but obviously also other hydroperoxides may be formed and thus reduce the oxygen concentration. We model both conjugated dienes, and other hydroperoxides using the same equations, albeit using slightly different reaction rate constants. Although not many experimental studies involved concomitant measurements of both markers (generally, only one is chosen), an indication of the relative reactivity towards conjugated dienes and hydroperoxides can be found in e.g., the work of (Allen, Jackson, & Kummerow, 1949; Kamal-Eldin, 2003; Okubanjo, Ye, Wilde, Singh, & Loveday, 2021; Viau, Genot, Ribourg, & Meynier, 2016). These authors studied oxidation of various bulk oils or emulsions, and measured conjugated dienes and total hydroperoxides at different stages. The ratios between these components depend greatly on the oil used, with most systems showing considerably higher total amounts of hydroperoxides compared to conjugated dienes. When directly translating these findings to the system that we investigate here, this may imply that the reaction rate constants for both components are similar. In the model we take the relative reactivity between conjugated dienes and other hydroperoxides as a constant. In the outlook section, the sensitivity of the model for the choice in relative reactivity is discussed further.

The number of double bonds available for reaction is calculated from the fatty acid composition reported in (Berton, Genot, & Ropers, 2011).

The number of double bonds present in all PUFAs is taken as one category, and added up into one overall concentration (4.5 mol/kg oil).

Because the initial amount of hydroperoxides other than conjugated dienes was not measured, it was calculated using the reactivity ratio, and the initial amount of conjugated dienes present at t = 0 using:

$$[\mathrm{LOOH}]_{\mathrm{otherHPOX},t=o} = [\mathrm{LOOH}]_{\mathrm{PUFA}} \bullet \left[\text{reactivity ratio}\right] \quad \text{(IX)}$$

A similar assumption was used for the secondary oxidation products; reactivity ratios were kept constant.

The oxygen concentration is expressed as mmol oxygen per kg oil, and based on the saturated concentrations at 25 °C in water (8.5 mg/L (Karbowiak et al., 2010; engineering toolbox)), in vegetable oil (45 mg/L (Cuvelier et al., 2017)), and on the amount of oxygen present in air (21 %). The total amount of oxygen in the reaction tubes is thus determined to be 154 mmol per kg oil.

The reaction rate equations are used to find parameter sets that describe lipid oxidation in the five emulsions simultaneously. This implies that rate constants related to reactions expected to take place *away* from the interface (k_2-k_4) are considered constant, whereas reactions related to radical formation at the interface (k_1 and k_5) are allowed to vary between emulsions, because of the different emulsifiers used.

As a starting point for parameter values related to radicals, we use the work of Kamal-Eldin (Kamal-Eldin, 2003). In Table 1.2 in that work, we found references to zero order rate constants expressed as 1/[s·M], for reaction 2 and 3 in our scheme. These values cannot be used directly because in our model first order reaction rate constants are used (unit is 1/s), but we can recalculate the parameter values originally reported by Babbs and Steiner, and Kasaikina and co-workers (Babbs & Steiner, 1990; Kasaikina, Kortenska, & Yanishlieva, 1999) into first order constants using the radical concentrations. We take the initial $L^\bullet$ and $LOO^\bullet$ concentrations equal to $2{\cdot}10^{-9}$ and $1{\cdot}10^{-10}$ M/L, respectively (see results), as given in (Babbs & Steiner, 1990), and later evaluate the effect of this choice on the overall course of reactions.

The procedure that was ultimately used is the following:

1. For both Tween-based emulsions, the effect of k_2 and k_3 variation on the maximum amount of conjugated dienes was evaluated, together with the effect on oxygen consumption.
2. Simultaneously k_5 was adjusted to position the lines that were generated by the model as close as possible to the measured points for conjugated dienes and oxygen.
3. Based on visual agreement of fit, the values of k_2, k_3 and k_5 were estimated.
4. These constants were used to predict the behavior of the protein-stabilized emulsions by adjusting both k_1 and k_4.
5. The parameter values (k_1-k_5) were determined based on visual agreement of fit (see Tables 1, and A1 in the supporting information for overviews).

It is good to point out that we also considered various other scenarios that did not lead to satisfying descriptions of the reaction, and share the insights gained since this is relevant to others that want to use the approach we describe.

(a) High k_1 values can be used to describe oxidation in protein-stabilized emulsions, but does so at the expense of very high concentrations of radicals (which is not realistic, due to their low to very low lifespan), and it does not lead to appropriate description of Tween-stabilized emulsions.
(b) The model with k_5 describes both the behavior of Tween-stabilized emulsions well (see results section), and to some extent that of the protein-stabilized emulsions can also be described, but for the latter this leads to very steep decrease in conjugated diene concentrations as soon as the oxygen is running out, which does not happen in practice.
(c) It was considered to use k_1-k_5 for all emulsions, but since k_1 is not needed to reach appropriate descriptions of the Tween-stabilized emulsions, and k_5 not for protein-stabilized emulsions; we kept the model as simple as possible and considered these constants zero in the respective emulsions, thus doing justice to Ockham's razor.

The main discussion in the results is about the comparison of these two scenarios. To be complete, we have added three graphs and a table with parameters for protein stabilized-emulsions in the supporting material in which we have used k_5-values as found for the Tween-stabilized emulsions, and adjusted the k_1-values to obtain descriptions that are in line with the experimental data points.

3. Results

3.1. Overall description of model predictions

The model allows us to predict the concentrations of oxygen, unreacted fatty acids, and oxidation products as function of time (see Fig. 2 for an example for a Tween 20-stabilized emulsion). We start by first showing a typical result as would be generated by the model, and in the next section compare with measured data.

As mentioned in the methods section, the model with which the Tween-stabilized emulsions were described only contains reaction rate constants (k_2-k_5). This implies that the oxidation reaction is initiated by the primary oxidation product (LOOH) that reacts to form a peroxyl radical $LOO^\bullet$ (k_5), or reacts on to a secondary oxidation product (k_4). This radical ($LOO^\bullet$) reacts with unoxidized fatty acids (LH/LH') to form a new alkyl radical $L^\bullet$ (k_3) and a new primary oxidation product (LOOH). Radical $L^\bullet$ reacts with oxygen (k_2) to form $LOO^\bullet$.

The amount of oxidizable PUFAs decreases slightly over the course of the reaction, but many remain after oxygen runs out, which confirms that the oxidizable lipid substrate is present in large excess. Conjugated dienes are being formed slightly faster than other hydroperoxides, and that is also the case for secondary oxidation products that form more readily from conjugated dienes, although the difference is not that great.

As will be demonstrated later, the model makes it possible to capture factors that generally are not considered when comparing results obtained for different emulsions, such as the effect of having different k_1's and k_5's that are both related to effects taking place at the oil–water interface. In essence such effects may be different in the emulsions studied here since they would have other interfacial composition, or differences in the amount of hydroperoxides that are initially present and drive reactions 4 and 5, as will be explained in greater detail in the next section. It is good to already point out that the model does not include any radical termination reactions, and may thus in some cases lead to high concentrations of radicals after the oxygen has run out.

To put our findings in a much broader perspective, the observed behavior (Fig. 1) is typical for cascaded reactions: depending on reaction rate constants and concentrations, various concentrations of components will be formed at different points in time, therewith influencing the rate at which all components are formed. In classic reactor design, the reaction rate constants would be taken to determine the maximum yield, or prevent the formation of undesired reaction products as much as possible. For the interested reader, we recommend the following books for chemical engineering (Westerterp et al., 1987), for bioreactor applications (Riet & Tramper, 1991), or previous work of one of us dealing with enzyme-catalyzed antibiotic synthesis (Schroën, Fretz, et al., 2002; Schroën, Nierstrasz, et al., 2002). In the current work, we zoom in on effects related mostly to oxygen consumption and conjugated diene formation.

3.2. Oxygen consumption and conjugated diene formation

In order to compare oxidation in the various emulsion, we use graphs

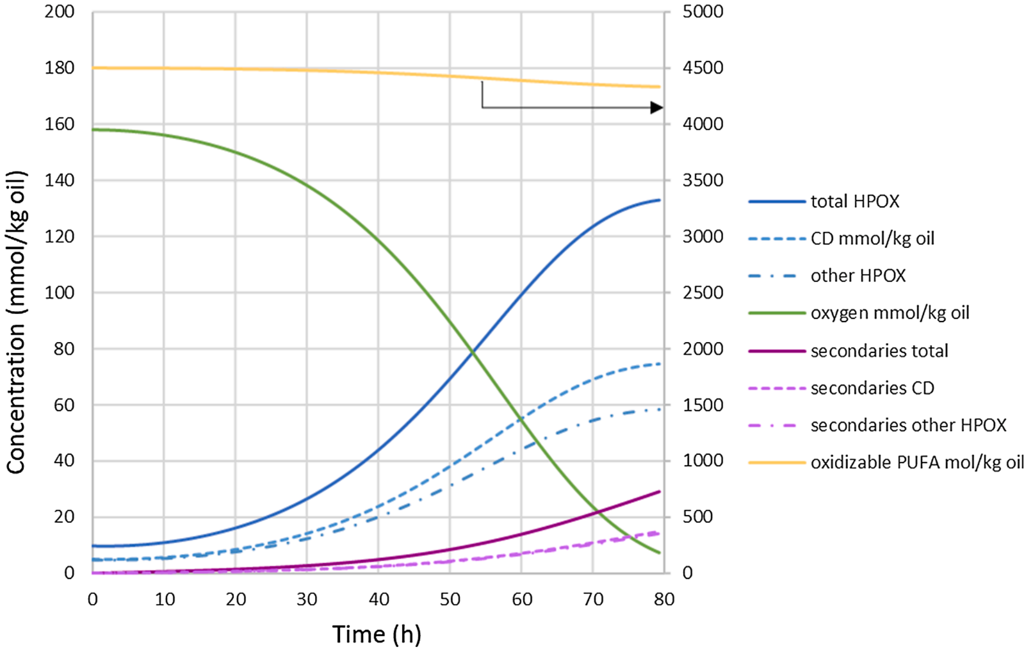

Fig. 2. Example of a modelling outcome for a Tween 20-stabilised emulsion, with substrate(s) and oxidation products represented. The yellow line denotes the oxidizable PUFAs with values on the right y-axis, all other concentrations are on the left y-axis (units are the same in both y-axes). Colors are similar for hydroperoxides (HPOX), and secondary oxidation products. Total amounts are shown through solid lines, dashed lines are for conjugated dienes, and products that are formed from them, dash-dotted lines are for other hydroperoxides, and reaction products formed from them. (For interpretation of the references to color in this figure legend, the reader is referred to the web version of this article.)

such as those in Fig. 3 in which oxygen, conjugated dienes, and total hydroperoxides are shown. Furthermore, the total secondary oxidation products are shown. We start by discussing the surfactant-stabilized emulsions; please keep in mind that the model only contains (k_2-k_5).

3.2.1. *Modelling Tween-stabilized emulsions*

The model is able to describe the reactions well: the actual parameters that are used are given in Table 1, right panel. From Fig. 3, it is clear that the amount of oxygen consumed and the amount of primary oxidation products formed varies between the emulsions. Since $k_2 - k_4$ (see also next section in which the parameter values are compared to expectations from literature, as well as the outlook section), are kept constant, this cannot explain the difference. The obvious difference is in the k_5 value used $3.3{\cdot}10^{-3}$ versus $2.5{\cdot}10^{-3}h^{-1}$, but what is less evident is that the initial amounts of conjugated dienes (primary oxidation products) are different for the two emulsions (7 mM for Tween 20-, and 5 mM for Tween 80-stabilized emulsions, respectively). In the Tween 20-stabilized emulsion, this drives the oxidation reaction to be faster than the one in the Tween 80-stabilized emulsion (see also supporting information A2 in which we systematically compare the effect of reaction rate constants as well as initial conjugated diene concentrations). Besides, the droplet size (d_{32} 1.4 vs 1.7 µm for Tween 20- and Tween 80-stabilized emulsions, respectively) is different. The ratio of droplet sizes and k_5-values is both around 1.3, which may imply that the two emulsions are actually obeying the same kinetic parameters, that is if the k_5-value is corrected for the specific surface area present. We have not done that because such aspects would first require a systematic investigation based on well-contrasted and controlled systems in terms of droplet size, but given the fact that the k_5-values relate to reactions initiated at the surface, this is a logical way to interpret the differences, and bring them to an even broader common ground.

It is also good to point out that the actual values of k_5 indicate that approximately 0.2–0.3 % of the hydroperoxides present undergo reaction 5 per hour. As mentioned in the introduction, LOOH reacts under the influence of Fe^{2+} that is oxidized to Fe^{3+}, that in turn reacts back to Fe^{2+}under the formation at LOH. Since the latter reaction is much faster,

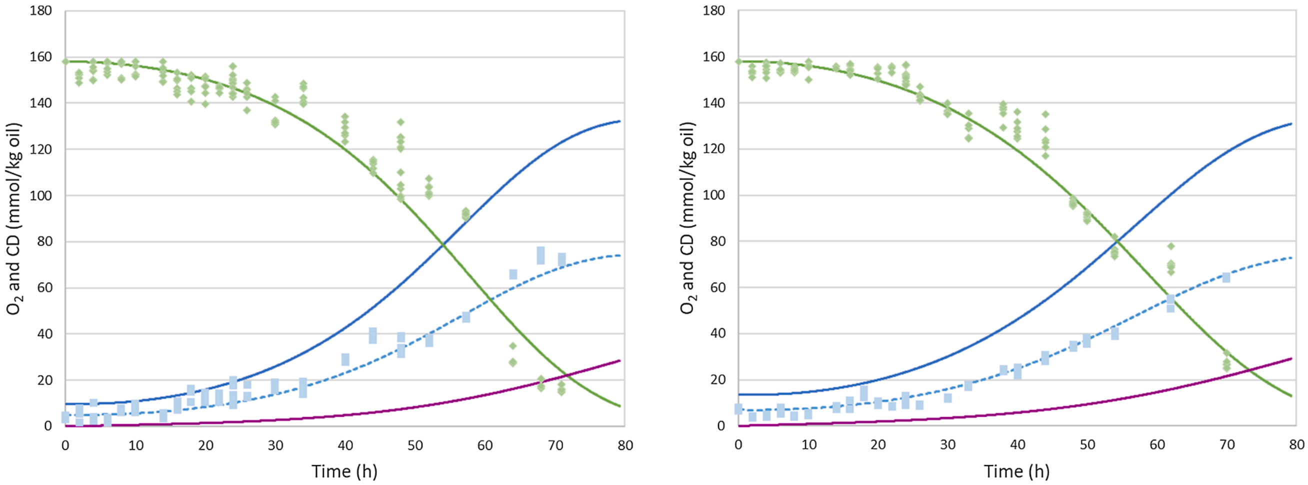

Fig. 3. Experimentally determined amounts of consumed oxygen (green diamonds), and produced conjugated dienes (blue squares), and the predicted values for oxygen concentration (green), conjugated dienes (blue dashed line), total hydroperoxides, and total secondary products (purple) in Tween-stabilized emulsions; left Tween 20, right Tween 80. (For interpretation of the references to color in this figure legend, the reader is referred to the web version of this article.)

Table 1
Overview of reaction rate constants related to conjugated dienes used in the model, for the different emulsions (the top row refers to the emulsifier used for each).

	β-lactoglobulin	Bovine serum albumin	β-casein	Tween 20	Tween 80
$k_{1,CD}$ (h^{-1})	$6.5\cdot10^{-5}$	$2.7\cdot10^{-5}$	$1.4\cdot10^{-5}$	–	–
$k_{2,CD}$ ((mol/kg oil) · h) $^{-1}$	10	10	10	10	10
$k_{3,CD}$ ((mol/kg oil) · h) $^{-1}$	1	1	1	1	1
$k_{4,CD}$ (h^{-1})	$6\cdot10^{-3}$	$6\cdot10^{-3}$	$6\cdot10^{-3}$	$6\cdot10^{-3}$	$6\cdot10^{-3}$
$k_{5,CD}$ (h^{-1})	–	–	–	$3.4\cdot10^{-3}$	$2.7\cdot10^{-3}$
$k_{propanal}$ (h^{-1})	$3.5\cdot10^{-4}$	$3.5\cdot10^{-4}$	$3.5\cdot10^{-4}$	$3.5\cdot10^{-4}$	$3.5\cdot10^{-4}$
$k_{hexanal}$ (h^{-1})	$6\cdot10^{-5}$	$6\cdot10^{-5}$	$6\cdot10^{-5}$	$6\cdot10^{-5}$	$6\cdot10^{-5}$
Initial $L^{\bullet}$ concentration (μmol/kg oil)	500	10	100	1	1
Droplet size (μm)	1.5	1.8	1.7	1.4	1.7

*All parameters related to other hydroperoxides are 0.95 (reactivity ratio) times those of conjugated dienes (full overview of parameters in the table in supporting information A1). Parameters that varied between emulsions are in italic script.

it can safely be assumed that the amount of reactive Fe^{2+} remains constant, and that the formed LOH needs to be the same as the amount of LOOH undergoing reaction 5, (0.3 %), which is so low that the reaction can be safely neglected in the overall reaction scheme.

There is quite a difference in how fast reactions proceed (see next section), and in most emulsions the formation of secondary oxidation products only just started (which would make it impossible to get adequate parameter values when only using one data set), which allows us to quantitatively compare the effects taking place in the various emulsions.

3.2.2. *Parameter value comparison*

Before going to a comparison of the reactions in the various emulsions, we first want to dedicate some words to the parameter values that are found, and how that relates to other parameters that are presented in literature (e.g., in (Babbs & Steiner, 1990; Kamal-Eldin, 2003; Kasaikina et al., 1999). As mentioned earlier, in these sources, rate constants are expressed as $M^{-1}\cdot s^{-1}$ and given for reactions 2 and 3 in our scheme. Direct use is not possible since the reaction rate constants used in our work are expressed as s^{-1}, but they can be converted into each other when concentrations are known or can be approached. The reported reaction rates related to k_2 were mostly in the order of 10^6 to 10^8 ($M^{-1}\cdot s^{-1}$) (Kamal-Eldin, 2003). When taking the radical concentration as 10^{-10} for $LOO^{\bullet}$, as reported in the modelling study of Babbs & Steiner (1990), this would lead to first order constants in the order of 10^{-4} – 10^{-2} s^{-1}, or when expressed per hour as being in the range of 0.3–36. The value that we found (10 h^{-1}) is right in the middle of this range. For k_3, a zeroth order rate constant of 31 ($M^{-1}\cdot s^{-1}$) was found in the work of Babbs & Steiner (1990), and a range of 40 ± 20 ($M^{-1}\cdot s^{-1}$) in the work of Kamal-Eldin (2003). Taking the concentrations in the paper of Babbs & Steiner that are typically between 0.01 and 0.05 mM hydroperoxides per litre oil, we calculate corresponding first order rate constants between 0.7 and 3.5 ((mol/kg oil)·h)$^{-1}$ when using 20 as the lowest value, or between 1.5 and 7 when using 40 which is the average value given in (Kamal-Eldin, 2003). These values were derived for 37 °C, whereas our experiments were carried out at 25 °C. In general the reaction rate constant would need to be decreased by a factor of 2–3 for every 10 °C temperature difference, which would correspond to an overall tentative interval for k_3 between 0.2 and 2.5 based on the literature mentioned previously. The value that we found (1) is within these ranges, which makes us confident that the values found are meaningful. Regarding the initial amounts of radicals that would be present in such emulsions, we expect them to be in the order of micromolar (Thomsen, Vedstesen, & Sikbsted, 1999). For the two surfactant-stabilised emulsions, we used 1 μM. For the reactivity ratio of conjugated dienes and other hydroperoxides, we found good agreement of fit for 95 % reactivity of the latter compared to CDs, and this value directly follows from the mass balances used. For a 100 % reactivity ratio, the oxygen would deplete faster than what was experimentally measured. In literature, mostly either CDs or hydroperoxides are reported, and only few have measured both. In the work of a number of authors (Allen et al., 1949; Kamal-Eldin, 2003; Okubanjo et al., 2021; Viau et al., 2016) done with similar vegetable oil emulsions, comparable reactivities were found for CDs and other hydroperoxides.

3.2.3. *Modelling protein-stabilized emulsions*

As was done for the Tween-stabilized emulsions, we modelled the lipid oxidation kinetics in the protein-stabilized emulsions, but now varied k_1 corresponding to direct $L^{\bullet}$ formation (as motivated in the Materials and methods section), and kept k_5 at zero. We again found very reasonable descriptions of the measured values (see Fig. 4 and Table 1, left three entries; for an overview of all reaction rate constants, please consult the supporting information, Table A1).

From the overall reaction behavior, it is clear that great differences exist between the emulsions (including the Tween-stabilized emulsions), here highlighted in the extent of primary oxidation product formation, and oxygen consumption. Still, the parameter values are remarkably the same, with only differences for k_1 which we interpret as being an effect of interface-related radical formation.

In literature, the effect of interfacial composition on oxidation has very rightly been pinpointed as highly influential on oxidation (Berton-Carabin et al., 2014; Coupland & Mcclements, 1996; Laguerre et al., 2017). The fact that the other reaction rates would not be affected beyond what kinetics dictates is a very new insight that could only be obtained through the full analysis that was carried out in the present work. It is also important to point out that our results show that there is no indication that mass transfer effects, or concentration gradients would play an important role, as is often argued in literature when comparing results. If they did, we would not have been able to describe the course of the reactions in the emulsions in such unified fashion. Whether this is the case only for the systems considered here (free-flowing emulsions, incubation under rotative agitation, acceleration of oxidation using a chemical initiator), or would be a more generic behavior in model and real food emulsions, would deserve further investigation.

Zooming in on k_1, it is clear that the β-lactoglobulin-stabilized emulsion has the highest k_1 value, with the BSA-based one having approximately 1/3rd of that value, and the casein-based one having 1/5th of the value of the β-lactoglobulin-stabilized emulsion. Lipid oxidation in the protein-stabilized emulsions is faster than in the surfactant-stabilized ones, that typically need more time to 'get up to speed' (please note the difference in times used in the experiments) but ultimately also consume all oxygen present. At this stage, high amounts of radicals are predicted by the model (see supporting information A1) because it does not include termination reactions. In reality the amounts of radicals are expected to be lower due to radical recombination reactions.

The initial radical amounts have been varied for the emulsions. There, where for both Tween-stabilized emulsions the initial radical concentration was taken at 1 μM, the radical concentrations for the protein-stabilized emulsions are considerably higher (as indicated in Table 1). The β-lactoglobulin-stabilized emulsion was used to evaluate the effect of initial $L^{\bullet}$ radial concentration. We systematically increased the concentration from 10^{-9} to values as high as 10^{-3} M/kg oil and found that the course of the reaction was not influenced till concentrations of ~ 10^{-5}. When exceeding this value, the reaction started to behave

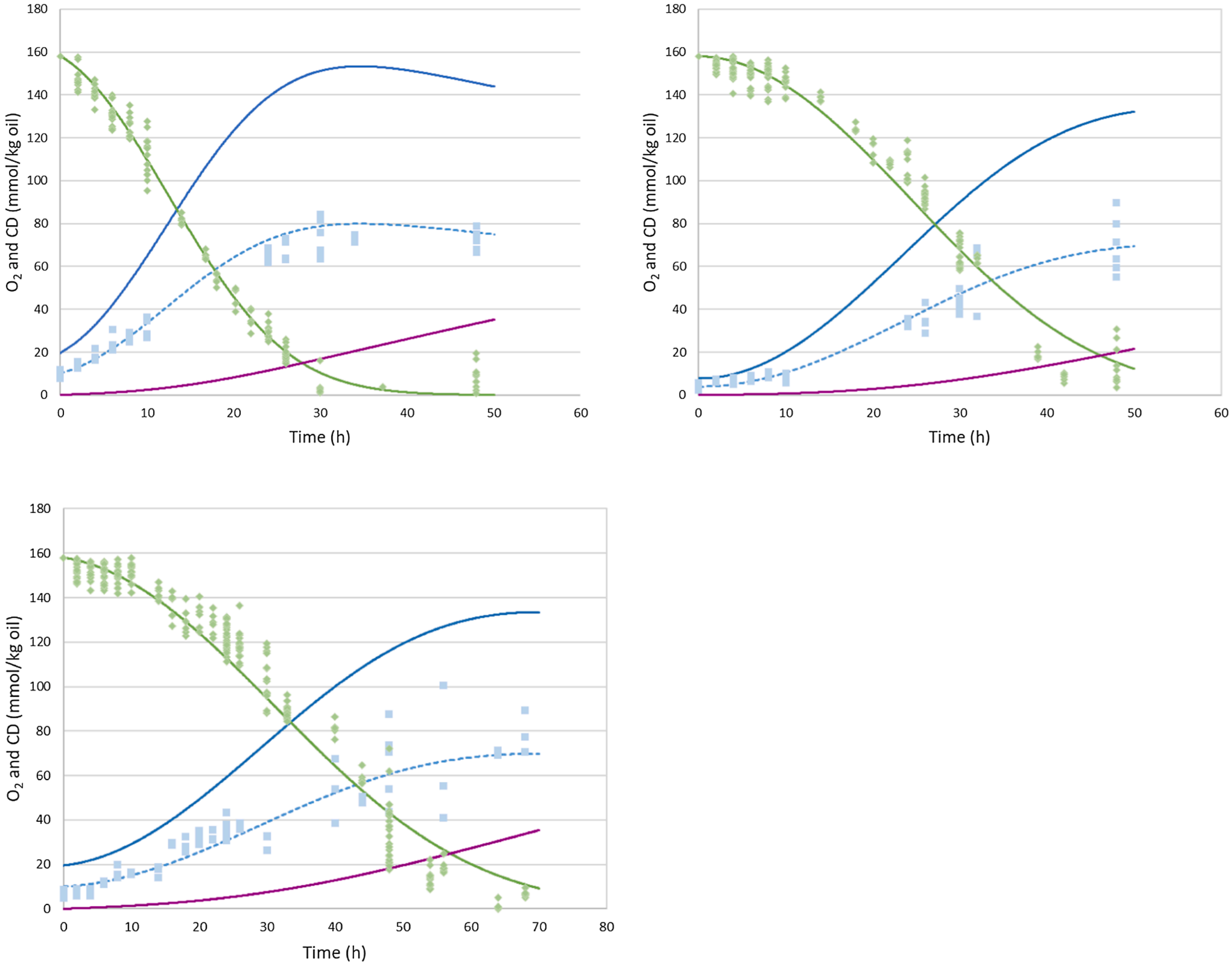

Fig. 4. Experimentally determined amounts of consumed oxygen (green diamonds), and produced conjugated dienes (blue squares), and the predicted values for oxygen concentration (green), conjugated dienes (blue dashed line), total hydroperoxides, and total secondary products (purple) in protein-stabilized emulsions. Emulsions are stabilised by β-lactoglobulin (top left), bovin serum albumin (top right), and β-casein (bottom). (For interpretation of the references to color in this figure legend, the reader is referred to the web version of this article.)

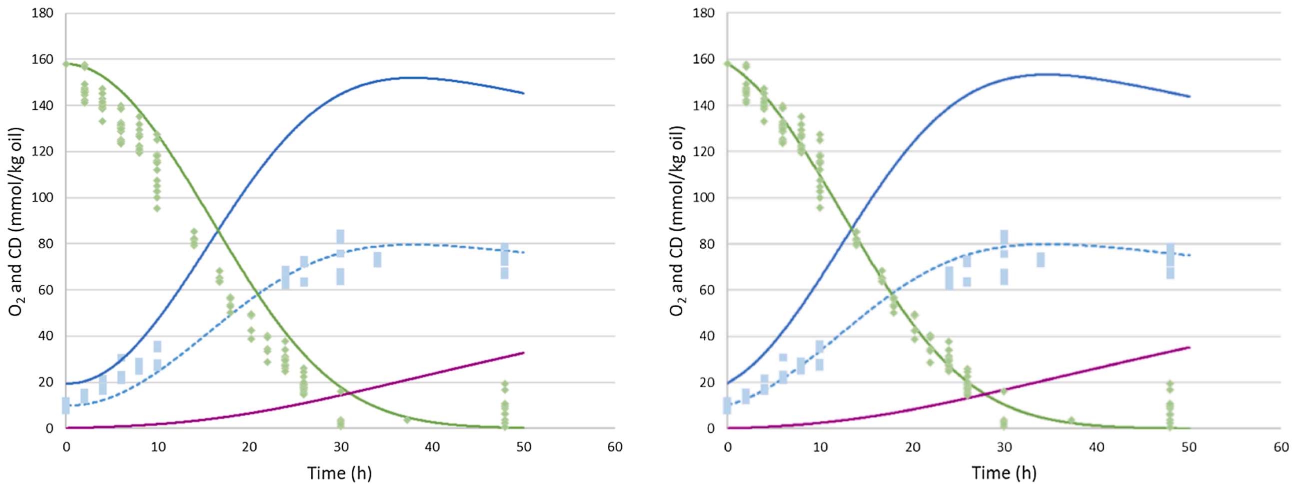

Fig. 5. Experimentally determined amounts of consumed oxygen (green diamonds), and produced conjugated dienes (blue squares), and the predicted values for oxygen concentration (green), conjugated dienes (blue dashed line), total hydroperoxides, and total secondary products (purple) in β-lactoglobulin-stabilized emulsions for intial $L^{\bullet}$ concentrations of 1 (left) or 500 μM/kg oil (right). (For interpretation of the references to color in this figure legend, the reader is referred to the web version of this article.)

slightly differently, especially in the initial phase as illustrated in Fig. 5 in which the initial radical concentration in the β-lactoglobulin-stabilized emulsion is increased from 1 to 500 μM/kg oil. The initial formation rate of conjugated dienes, and oxygen consumption rate are quite rapid for the highest radical concentration and in much better agreement with the measured values. Whether this also implies that the emulsion holds this initial radial concentration cannot be confirmed with the available experimental data from Berton et al. (2011), and it should be pointed out that due to their high reactivity, alkyl radicals are in essence difficult to measure.

The estimated initial concentrations of $L^\bullet$ radicals vary between the different protein-stabilized emulsions, with the β-lactoglobulin-based one needing the highest concentrations to achieve good descriptions as elaborated above, the β-casein-based one showing the second highest concentration (100 μM/kg oil), and the BSA-stabilized emulsion having the lowest among all three protein stabilized-emulsions (10 μM/kg oil), but still exceeding both Tween-stabilized emulsions for this criterion, with a factor of 10. We expect that the emulsification process (high pressure homogenization) may have induced lipid radical formation due to cavitation phenomena. On top of that, adsorbed proteins may induce additional radical formation that is known to influence lipid oxidation. In fact, the proteins in these emulsions were measured to be themselves subject to extensive oxidation (Berton et al., 2012), and since it is known that protein oxidation can induce lipid oxidation, and vice versa (Berton, Ropers, Guibert, et al., 2012), this is a logical explanation for our observations, which is also in line with findings of others for various systems (Estévez, Kylli, Puolanne, Kivikari, & Heinonen, 2008; Merkx et al., 2021; Østdal, Davies, & Andersen, 2002; Salminen, Heinonen, & Decker, 2010; Yang, Verhoeff, Merkx, van Duynhoven, & Hohlbein, 2020). For our emulsions this leads to an overall effect that can differ greatly (a factor of 50 is found within the proteins, and a factor of 500 if also Tween is included), as is also evident from the images in Figs. 3 and 4.

In spite of all the differences that we have discussed, it is of utmost importance to point out that the basis for the lipid oxidation behavior in all emulsions is the same, and that is what we now are uncovering using our modelling approach. Before discussing this in greater detail, we first present the formation of secondary lipid oxidation products.

3.3. Secondary lipid oxidation products

The secondary oxidation products are formed throughout the incubation period, although they only start forming in substantial amounts when the concentration of the primary oxidation products reaches a certain level. Please keep in mind that k_4 corresponds to the formation of all secondary oxidation products (Table 1), not just to hexanal and propanal, that are both formed to a much lesser extent. The corresponding constants in Table 1 can be interpreted as a percentage of the total aldehydes formed related to k_4 (7 % and 1.2 %, for propanal and hexanal, respectively).

When comparing the predictions for propanal and hexanal concentrations (Fig. 6), we see reasonable agreement with the measured values. Also here, we note the variation in the measured values as was the case earlier when describing oxygen consumption and primary oxidation product formation, which also greatly affects the visual impressions. At high concentrations, the measured values are on the low side, and this could be caused by saturation of the solid state adsorption fiber used to capture volatiles (Berton, Genot, Viau, et al., 2011). Still, we feel that given the very general approach that we chose, the agreement between measured values and model is good.

3.4. Overall interpretation of the reactions and the effect of emulsifiers

From the previous sections, we conclude that it is possible to define a very general basis for lipid oxidation when comparing with data that are obtained under conditions that are free of mass transfer limitations, and are not affected by sampling (see next section). The results prominently highlight the role of the two radical formation reactions related to k_1 and k_5. It is generally accepted that these effects are related to the interface of the emulsion and to the components that are present.

When discussing the Tween-stabilized emulsions earlier on, there is potentially a droplet size effect on k_5. The droplet size of the emulsions before and after incubation are reproduced below in Table 2 (Berton, Genot, Viau, et al., 2011), and in general, the emulsions have been rather physically stable, and have comparable droplet sizes, although some differences can be noted. If the oxidative reactions were only related to the amount of surface area, all emulsions would have had very similar oxidation rates. Based on the droplet size, the difference in surface is at most of 30 % initially. For the protein-stabilized emulsions, the k_1 values are a factor of ∼ 5 different and that makes us conclude that it is not the specific surface area as such that determines the oxidation reaction in protein-stabilized emulsions, but the composition of the interface most probably through differences in iron binding and chelating properties.

To illustrate the effect of different parameter values on the model outcomes, we have put a number of scenarios in Fig. 7. Most graphs relate to the Tween 80-based emulsion for which k_2-k_5 were varied, and also the initial hydroperoxide concentration by taking 50 % of the actual value, and increasing it with 50 %, which allows us to investigate the sensitivity of the model for parameter differences. For the β-lactoglobulin-based emulsion, we only varied k_1. The reference system is always in the middle panel.

From all these parameter adjustments and corresponding graphs, it is clear that the course of the reactions is very sensitive to variation of k_1, k_2, and k_5, as well as to the initial hydroperoxide concentration. Earlier we also pointed out the sensitivity to the initial lipid radical concentration. These are all effects that relate to the initial stages of the lipid oxidation reaction, thus stressing the importance of the starting point of the cascaded reaction of which the later stages are a logical consequence. The model seems much less sensitive to variation of k_3 and k_4. Since there is not that much aldehyde formed from a molar concentration perspective, it is logical that the reaction related to k_4 would not be that greatly affected by this value, but for k_3 which is the reaction leading to LOOH, we find this remarkable. Apparently, this reaction is not the overall rate-determining step in the overall scheme.

Finally, we would like to briefly discuss what the effect of using k_5 in the model to describe oxidation in protein-stabilized emulsions would be. We decided to use k_5-values that are the same as found for the Tween-stabilized emulsions, depending on the size of the droplets, and have adjusted the k_1-values in such a way that again a good description was obtained (see supporting information, Figure A2, and Table A2). When comparing these figures with those in the main text, it is clear that they both give very reasonable descriptions of the course of the reaction, and they cannot be distinguished based on goodness of fit since they are both really good.

From a comparison between the original k_1 values, and the ones in table A2, it is clear that adding hydroperoxide radical initiation at a level as expected to occur in surfactant-stabilized emulsions leads to considerable reduction in k_1, illustrating the possible impact of this reaction. The main effect is still created by k_1 in emulsion stabilized by β-lactoglobulin and BSA, while for β-casein the main effect would be coming from k_5 when occurring at the level as found in Tween-stabilized emulsions. Whether hydroperoxide-based radical initiation needs to be added to describe protein-stabilized emulsions is currently under investigation; for now we keep the number of parameters as low as possible for our interpretation of results, as is a good custom in modelling in general. To be complete, it was checked if the initial radical concentration needed to be kept at the same level as stated before when using five parameters, and that is indeed the case.

4. Outlook

We are very aware that we have chosen experiments carried out

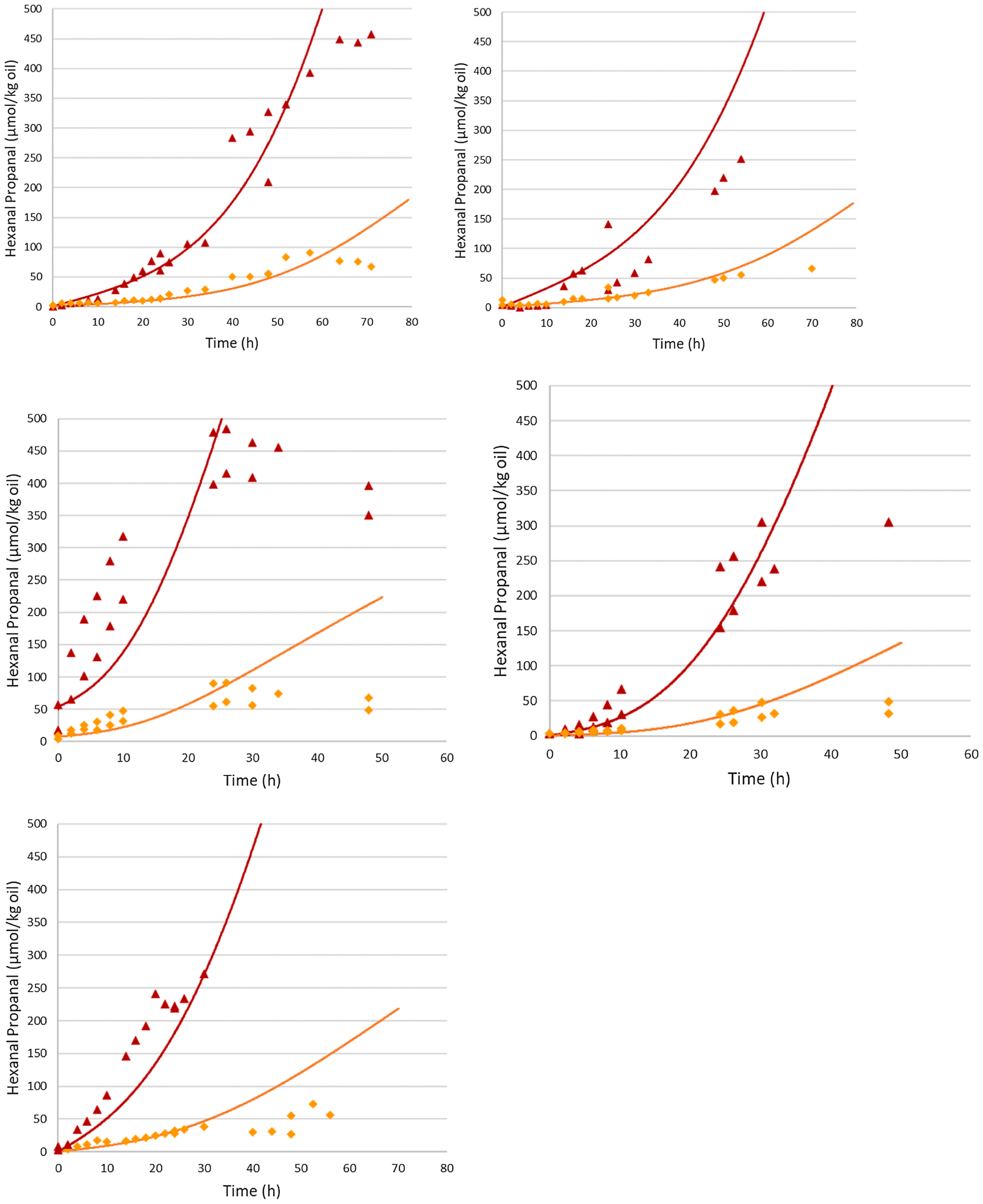

Fig. 6. Propanal (red triangle) and hexanal (orange diamond) formation as measured in the five emulsions together with the model predictions as solid lines of the corresponding color. Top line, left Tween 20, right Tween 80, middle line, left β-lactoglobulin, right bovine serum albumin, bottom, β-casein. (For interpretation of the references to color in this figure legend, the reader is referred to the web version of this article.)

Table 2
Emulsion droplet size. Reproduced from Berton et al. (2011), with permission of ACS Publications.

Emulsifier	D_{32} (t = 0) [μm]	D_{32} (t = 48 h) [μm]
β-lactoglobulin	1.5 ± 0.1	2.1 ± 0.1
Bovine serum albumin	1.8 ± 0.1	2.0 ± 0.1
β-casein	1.7 ± 0.1	1.7 ± 0.1
Tween 20	1.4 ± 0.1	1.3 ± 0.1
Tween 80	1.7 ± 0.1	1.6 ± 0.1

under highly controlled conditions, and this has allowed us to establish the general basis that we present. We feel that the fact that many data points could be used, have made it possible to draw the conclusions that we made. In literature, often very limited points are used, and limited components are measured, and when seeing that in the light of the variability of the curves in Fig. 6, it is clear that depending on the timepoints used, it will not be possible to draw clear conclusions (although this is still often done). We also want to be critical about the choices that we have made, and link to experiments that may be carried out under different conditions.

4.1. Oxidation initiator and bulk effects

For the experiments that we modelled, we used an iron-based oxidation initiator, which is a well-motivated choice in lipid oxidation research (Berton, Ropers, Bertrand, Viau, & Genot, 2012; Schaich, 1992). It does allow for relative control over the reaction, and this may be rather different when initiating the reaction in a different way (Berton et al., 2012). Furthermore, it is well-known that any emulsifier that is still present in the bulk phase will influence oxidation initiation; e.g. proteins are known to bind iron. In previous work by one of us (CCBC) one decade ago, this was demonstrated experimentally (Berton, Genot, Viau, et al., 2011). When comparing this result with our model, we find a substantially lower value for k_1 in case of protein-stabilised emulsions (while keeping the other parameters the same). For the Tween-stabilized emulsions, adjustment of k_5 is needed to capture this effect, but the rest of the constants can be kept as defined previously (results not shown). This seems to indicate that additional surfactant/protein in the bulk phase most probably influences the concentration of initiator at the interface (Villeneuve et al., 2021). Others have also suggested that the interface may become less permeable for iron and thus reduce the oxidation reaction, but we find this less likely.

4.2. Substrate choice and incubation conditions

We have decided to work with an oil that is rather unsaturated, and have used it at 30 % in the emulsion. This allows the emulsion to flow freely, with mass transfer taking place freely as well (all emulsions were incubated under slow rotative agitation). The molar ratio of oxygen to oxidizable bonds was rather low (1:30 approximately), which implies that all the oxygen can react. These conditions allow us to monitor the initial stage of the reaction well because we measure the substrate (O_2) of the reaction directly. This is not done very often, but we feel that in terms of modelling it is imperative to do so, since lipid oxidation products only appear after a number of reactions have already taken place, and these lipid radicals are extremely hard to measure. Insights into oxygen consumption may thus lead to insights in the very early stages of oxidation, even before considerable amounts of lipid oxidation products are formed, but in order for that to become a reality highly accurate measurement methods (i.e., with low detection and quantification thresholds) would need to become available. This takes the focus of the investigation to a very different level compared to what is customary done, using lipid oxidation products as the main target of investigation, and often allowing a so-called 'lag-time' during which seemingly nothing would happen (Bravo-Díaz, 2022; Pinchuk & Lichtenberg, 2014), but that is far from what is happening, as we were able to substantiate in the current paper. The oxidation products slowly but surely increase in concentration due to the overall kinetics that rule the reaction, and depending on the detection level of a method, this may be interpreted (falsely) as a lag time.

When investigating reaction kinetics through oxygen concentration, the use of gas tight containers is essential. It is strongly recommended to use sample vials only for one measurement in time, and not open them for repeated sampling. In doing so, oxygen would be replenished allowing the reaction to proceed, which in itself is not a problem and would give information for a more practical situation with a consumer repeatedly opening a jar, but does hamper determination of reaction rate constants to such an extent that this is no longer possible. As a last point of attention, under oxidative conditions, an under pressure will form in the headspace, and that may result in gas transfer into the incubation vessel if not gas tight, which will again allow the reaction to proceed beyond what would be possible based on the initial concentrations present. As mentioned in the methods section, we also adjusted the measured oxygen concentrations to do justice to the fact that when a sample is taken from the incubation bottle, air would flow into the sampling syringe, thus increasing the concentration of oxygen leading to underestimation of the oxygen consumption rate by 21 % (the amount of oxygen in the air). Current developments that allow the use of oxygen sensors in the vessel will mitigate these issues, provided they are sufficiently accurate, as mentioned earlier.

In the emulsions that we modelled in the current paper, a lot of care was taken to remove antioxidants by stripping with alumina. It is good to point out that in many practical emulsions, and also model emulsions presented in literature, indigenous chain-breaking antioxidants, or antioxidants that are added on purpose will be present. They would normally be 'consumed' by oxidizing themselves via H donation (forming antioxidant radicals, AH → A●). For oil soluble antioxidants, these reactions can be added to the scheme if needed. This step is part of future research.

In practice, often open containers are used thus keeping the oxygen concentration constant. In that case it is important to choose the product (oil, emulsions) layer thickness in such a way that no mass transfer limitations occur (as also elaborated on in the next section), and thus data on reaction kinetics are obtained that are not obscured by mass transfer effects. Especially in the work of Farhoosh (Farhoosh, 2018, 2020), considerable attention is paid to this, leading to reproducible measurements.

In principle, the model can now be used to compare various reaction conditions, so different oxidizable fatty acids to oxygen ratios, different oil fractions in the emulsion, different ratio of reactivity between conjugated dienes and other hydroperoxides, etc. This will be very instrumental when comparing data obtained in different labs, that at first sight may look very different, as did our results, but may have much more in common than thought.

4.3. Use of dimensionless numbers, diffusion distances and mixing

In the introduction, we have used dimensionless numbers to characterize our reaction systems, and could conclude that the considered emulsions behave as if they were ideally mixed systems that are free of mass transfer limitations. Here we shortly recall the principles underlying the Damköhler number, and Fick's law.

In the Damköhler number, a first order reaction rate constant needs to be used. In our system, only k_1, k_4 (and the k's related to propanal and hexanal), and k_5 qualify as such. We picked the highest k for our evaluation which is k_4, and find that Damköhler II is in the order of 10^{-7}-10^{-5}, so much smaller than 1 when using the droplet size as a characteristic size. This also implies that for droplets that are typically 10 times larger than here, this is still the case, but for droplets that are 100 times larger, the system can no longer be automatically considered as reaction-dominated. Obviously, this also holds for oil when present as layers

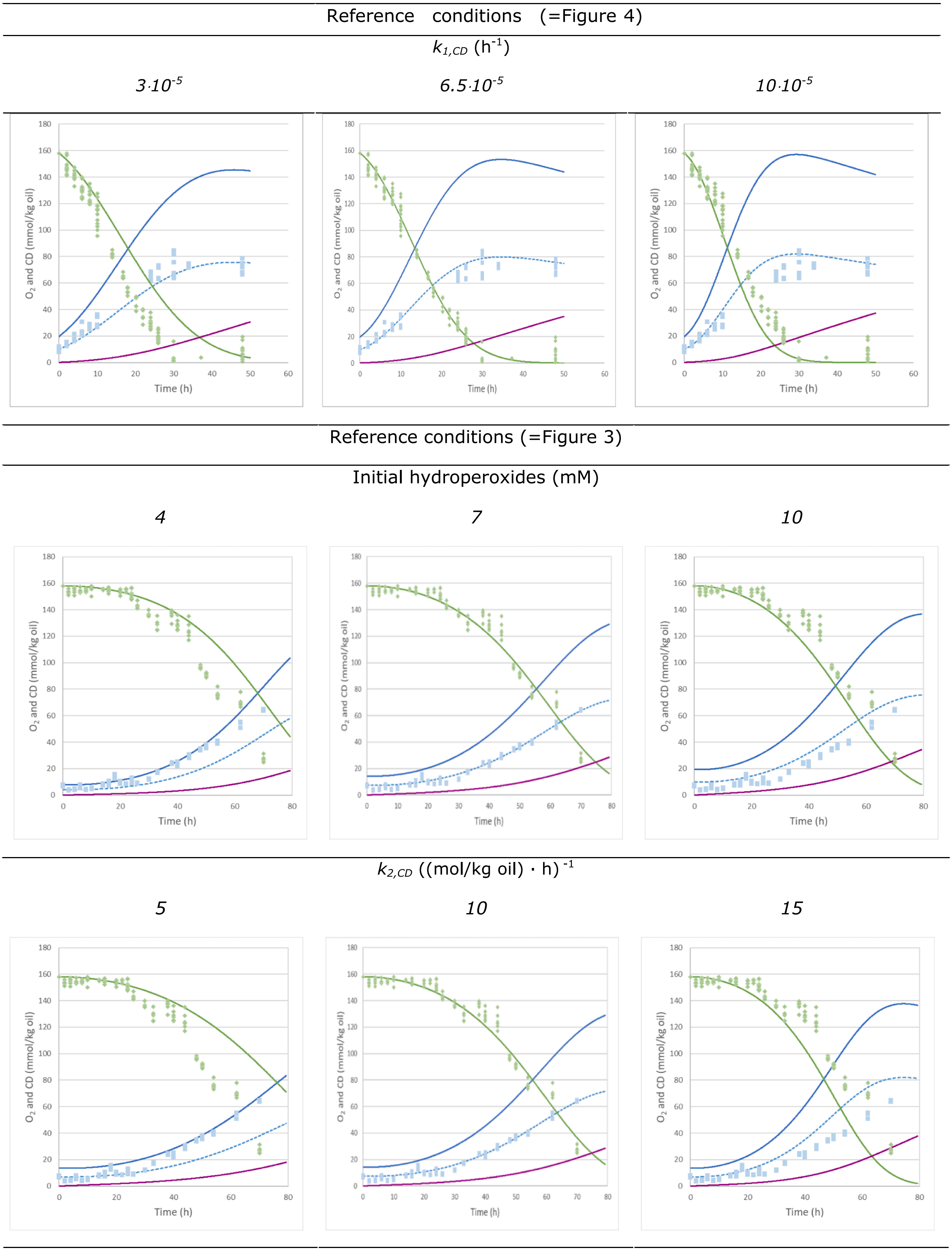

Fig. 7. Systematic parameter variation (+/- 50% of reference value) using the Tween 80-stabilized emulsion for k_2-k_5 and initial hydroperoxide variation, and the β-lactoglobulin-stabilized emulsion for k_1-variation.

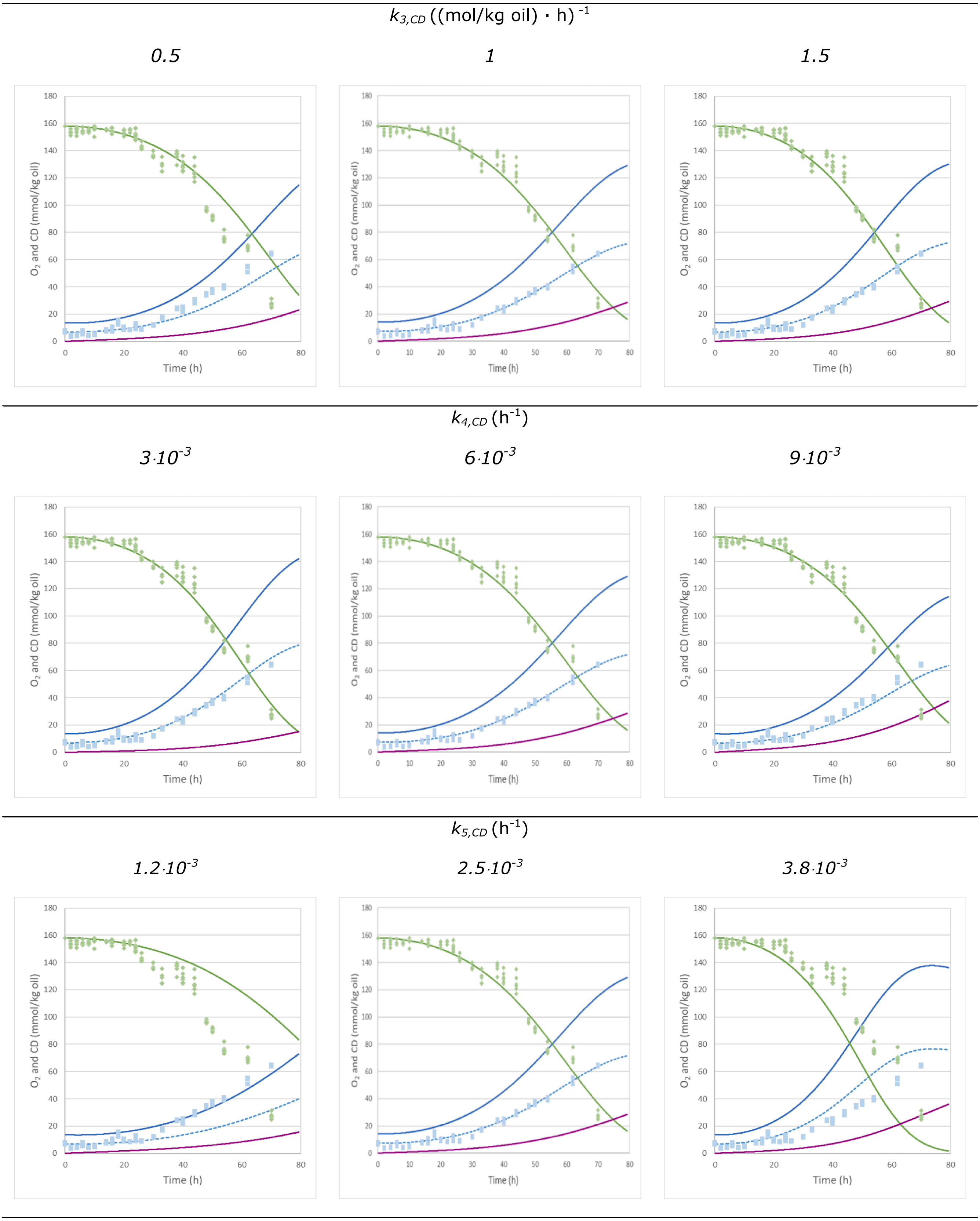

Fig. 7. (*continued*).

that exceed the aforementioned droplet dimensions.

Fick's law can also be used to evaluate various effects, and we have used it to compare an emulsion that is standing still (immobile tubes) compared to one that is continuously mixed. The characteristic dimension in a well-mixed system is the droplet size, and as mentioned earlier, diffusion of oxygen and triglyceride molecules will take place rapidly (within milliseconds, and within a minute, respectively). When using the height of the emulsion in a sample tube instead (around 10 cm), as would be the case for a still-standing incubation, the time needed for oxygen to diffuse from the headspace to the bottom of the emulsion would typically be in the order of hundreds of hours (practically all of the oxygen would be in the headspace, and not in the emulsion itself). Needless to say that incubation carried out in this way will lead to reactions that are severely limited by mass transfer, and these effects would need to be added to the current reaction kinetics basis that we established, in order to be able to describe these systems too. A lot of modelling approaches are available for this in the chemical, and biochemical engineering literature.

4.4. *Practical food emulsions*

The emulsions that we probed within this work are free-flowing, but obviously in practice many more examples of food emulsions are available, including high internal phase emulsions (HIPEs) such as mayonnaise, and even dried emulsions (Barden & Decker, 2016). For HIPEs, amongst others, it has been suggested that mass transfer between droplets plays and important role, and this has also been mentioned for low internal phase emulsions (Laguerre et al., 2017). Although we expect that such effects occur, our model does not indicate that they would be of great relevance for the relatively short reaction times and the low concentrations of surfactants in the bulk phase that were used in the emulsions studied here. Most of the components that are formed (e.g., hydroperoxides in triacylglycerols) are still of a high molecular weight and not likely to partition to other phases given their hydrophobic nature. We expect that lower molecular weight, more polar components will have a higher propensity to transfer, but these would typically be formed much later in the oxidation reaction.

In dried emulsions, the situation is expected to be even more extreme, since many components get ‘frozen in space’ when transformed into the typic glassy matrix of such products. Still, we expect that the effects that we describe presently can be relevant. The droplets will be exposed to a certain amount of pro-oxidants at the interface, leading to the cascaded reactions described earlier. It is expected that the drying process will induce considerable amounts of oxidation products upon preparation, which can very easily be incorporated in the model by adjusting the starting concentrations, as would be the case for any emulsion that contains oxidation products.

4.5. *Further use of the model*

The framework that we now have established will be useful to compare oxidation in emulsions as reported in literature. Obviously, many different incubation conditions can be used in practice, including different ratios between the substrate concentrations (oxygen and oxidizable oil), which is part of future work, and that will help solidify our approach further. It will also be possible to predict reactions when other oils are used by adjusting the amount of oxidizable fatty acids. When using other temperatures, parameters will need to be adjusted according to their temperature-sensitivity, which typically is in the order of a factor of 2–3 per 10 °C temperature difference.

It is good to point out that many variations can now be investigated systematically, and differences between emulsions can be quantified, not just based on points in time that were chosen ‘at random’, but through a full reaction course analysis. This will greatly contribute to overall understanding of lipid oxidation in emulsions, thus doing full justice to the interwoven effects of this cascaded reaction.

5. Concluding remarks

Using highly controlled conditions, and analysing specific components in time (substrates of the reaction, and reaction products), it is possible to develop a general scheme that describes the kinetics of the lipid oxidation reaction in time, thus doing full justice to the interconnectivity of all reactions that we considered. The scheme that we used is based on the reaction pathways classically described, and the actual parameters that we found and are in accordance with what others have found also for radical reactions.

We found that initiation of radials at the interface drives the reactions, and that all other parameters are similar for all emulsions. In Tween 20- and Tween 80-stabilized emulsions, initiation was explained by the decomposition of hydroperoxides into lipid radicals, whereas in protein-stabilized emulsions this was related to direct alkyl radical formation at the interface. Because of differences in capacity to initiate this reaction by the proteins, and the initial amounts of radicals present, the resulting course of the reaction was very different. The model is highly sensitive to differences in initial conjugated diene and other hydroperoxide concentrations, the reaction rate constants related to the previously mentioned initiation reactions, and that of the reaction of alkyl to peroxyl radicals, but much less sensitive to variation of the reaction rate constants related to the formation of primary and seconday oxidation products.

Based on the insights obtained, we were able to define guidelines that embrace insights from the field of chemical engineering that allow for fast evaluation of the reaction conditions and whether they are hampered by mass transfer limitations. An old saying in that field is reaction + diffusion = confusion, and we hope to have contributed to deconvoluting this at least partly for the field of lipid oxidation. The developed model is expected to be of great help in distinguishing between effects that are truly a result of reaction kinetics and of mass transfer effects.

Conception and availability of the model.

The model presented in this paper is the fruit of a ‘weekend’ project dedicated to finding out if a classic chemical engineering approach would help in understanding oxidation in emulsions. We are delighted with the outcome, and hope that many will work with the model. To make this as easy as possible, we have opted to use Excel (Microsoft) as a software. The model is available upon request.

Internet sources (all consulted in March 2022):

https://www.engineeringtoolbox.com.

https://www.biochemical-pathways.com.

Declaration of Competing Interest

The authors declare that they have no known competing financial interests or personal relationships that could have appeared to influence the work reported in this paper. The work was done out of interest and not funded through any project or program.

Appendix A. Supplementary data

Supplementary data to this article can be found online at https://doi.org/10.1016/j.foodres.2022.111621.

References

Allen, R. R., Jackson, A., & Kummerow, F. (1949). Factors which affect the stability of highly unsaturated fatty acids. I. Differences in the oxidation of conjugated and nonconjugated linoleic acid. *Journal of the American Oil Chemists' Society, 26*(8), 395–399.

Babbs, C. F., & Steiner, M. G. (1990). Simulation of Free Radical Reactions in Biology and Medicine : A New Two-Compartment Kinetic Model of. *Biomedical Engineering, 8*, 471–485.

Barden, L., & Decker, E. A. (2016). Lipid Oxidation in Low-moisture Food : A Review Lipid Oxidation in Low-moisture Food : A Review. *Critical Reviews in Food Science and Nutrition, 8398*. https://doi.org/10.1080/10408398.2013.848833

Berton-Carabin, C. C., Ropers, M. H., Guibert, H., Solé, V., & Genot, C. (2014). Lipid oxidation and related protein modifications in oil-in-water emulsions. San Antonio, Texas, U.S.A. Retrieved from http://edepot.wur.nl/326167.

Berton, C., Genot, C., & Ropers, M.-H. (2011). Quantification of unadsorbed protein and surfactant emulsifiers in oil-in-water emulsions. *Journal of Colloid and Interface Science, 354*(2), 739–748. https://doi.org/10.1016/j.jcis.2010.11.055

Berton, C., Genot, C., Viau, M., & Genot, C. (2011). Contribution of the Interfacial Layer to the Protection of Emulsified Lipids against Oxidation. *Journal of Agricultural and Food Chemistry, 59*, 5052–5061. https://doi.org/10.1021/jf200086n

Berton, C., Ropers, M. H., Bertrand, D., Viau, M., & Genot, C. (2012). Oxidative stability of oil-in-water emulsions stabilised with protein or surfactant emulsifiers in various oxidation conditions. *Food Chemistry, 131*(4), 1360–1369. https://doi.org/10.1016/j.foodchem.2011.09.137

Berton, C., Ropers, M. H., Guibert, D., Solé, V., & Genot, C. (2012). Modifications of interfacial proteins in oil-in-water emulsions prior to and during lipid oxidation. *Journal of Agricultural and Food Chemistry, 60*(35), 8659–8671. https://doi.org/10.1021/jf300490w

Van Boekel, M. A. J. S. (2001). *Reviews Kinetic aspects of the Maillard reaction : a critical review, 45*(3), 150–159.

Bravo-Díaz, C. (2022). Advances in the control of lipid peroxidation in oil-in-water emulsions: Kinetic approaches. *Critical Reviews in Food Science and Nutrition*, 1–33. https://doi.org/10.1080/10408398.2022.2029827

Calder, P. C. (2021). *Health benefits of omega-3 fatty acids. Omega-3 Delivery Systems*. Elsevier Inc. https://doi.org/10.1016/b978-0-12-821391-9.00006-5.

Callaghan, P. T., & Jolley, K. W. (1980). Translational motion in the liquid phases of tristearin, triolein, and trilinolein. *Chemistry and Physics of Lipids, 27*, 49–56.

Chaprenet, J., Berton-Carabin, C. C., Elias, R., & Coupland, J. (2014). Effect of interfacial properties on the reactivity of a lipophilic ingredient in multilayered emulsions. Retrieved from *Food Hydrocolloids, 42*(part1), 56–65 http://edepot.wur.nl/326081.

Chung, C., & McClements, D. J. (2014). Structure-function relationships in food emulsions: Improving food quality and sensory perception. *Food Structure, 1*(2), 106–126. https://doi.org/10.1016/j.foostr.2013.11.002

Conte, L., Milani, A., Calligaris, S., Rovellini, P., Lucci, P., & Nicoli, M. C. (2020). Temperature Dependence of Oxidation Kinetics of. *Foods, 9*, 294.

Coupland, J. N., & Mcclements, D. J. (1996). *food emulsions, 71*(March), 944–948.

Cuvelier, M., Soto, P., Courtois, F., Broyart, B., & Bonazzi, C. (2017). Oxygen solubility measured in aqueous or oily media by a method using a non-invasive sensor. *Food Control, 73*, 1466–1473. https://doi.org/10.1016/j.foodcont.2016.11.008

Erramreddy, V. V., Tu, S., & Ghosh, S. (2017). Rheological reversibility and long-term stability of repulsive and attractive nanoemulsion gels. *RSC Advances, 7*(75), 47818–47832. https://doi.org/10.1039/c7ra09605d

Estévez, M., Kylli, P., Puolanne, E., Kivikari, R., & Heinonen, M. (2008). Fluorescence spectroscopy as a novel approach for the assessment of myofibrillar protein oxidation in oil-in-water emulsions. *Meat Science, 80*(4), 1290–1296. https://doi.org/10.1016/j.meatsci.2008.06.004

Farhoosh, R. (2018). Reliable determination of the induction period and critical reverse micelle concentration of lipid hydroperoxides exploiting a model composed of pseudo-first and -second order reaction kinetics. *Lwt, 98*(July), 406–410. https://doi.org/10.1016/j.lwt.2018.09.003

Farhoosh, R. (2020). A reconsidered approach providing kinetic parameters and rate constants to analyze the oxidative stability of bulk lipid systems. *Food Chemistry, 327* (May), Article 127088. https://doi.org/10.1016/j.foodchem.2020.127088

Ghnimi, S., Budilarto, E., & Kamal-Eldin, A. (2017). The New Paradigm for Lipid Oxidation and Insights to Microencapsulation of Omega-3 Fatty Acids. *Comprehensive Reviews in Food Science and Food Safety, 16*, 1206. https://doi.org/10.1111/1541-4337.12300

Holman, R. T., & Elmer, O. C. (1947). The rates of oxidation of unsaturated fatty acids and esters. *J Am Oil Chem Soc, 24*, 127–129.

Jacobsen, C. (1999). Marcuse Lecture Sensory impact of lipid oxidation in complex food systems *. *Fett/Lipid, 101*(12).

Johnson, D. R., & Decker, E. A. (2015). The Role of Oxygen in Lipid Oxidation Reactions : A Review. *Annual Review of Food Science and Technology, 6*, 171–190. https://doi.org/10.1146/annurev-food-022814-015532

Kamal-Eldin, A. (2003). *Lipid Oxidation Pathways*. Champaign, Illinois: AOCS press.

Karbowiak, T., Egis, R., Gougeon, D., Alinc, J., Brachais, L., Ed, F. R., … Ee, A. (2010). Wine Oxidation and the Role of Cork. *Critical Reviews in Food Science and Nutritio*, *52*, 20–52. https://doi.org/10.1080/10408390802248585.

Kasaikina, O. T., Kortenska, V. D., & Yanishlieva, N. V. (1999). Effects of chain transfer and recombination/disproportionation of inhibitor radicals on inhibited oxidation of lipids. *Russian Chemical Bulletin, 48*(10), 1891–1896. https://doi.org/10.1007/BF02494742

Laguerre, M., Bily, A., Roller, M., & Birti, S. (2017). Mass Transport Phenomena in Lipid Oxidation and Antioxidation. *Annual Review of Fluid Mechanics, 8*, 391–411. https://doi.org/10.1146/annurev-food-030216-025812

Laguerre, M., Tenon, M., Bily, A., & Birti, S. (2020). Toward a Spatiotemporal Model of Oxidation in Lipid Dispersions. *A Hypothesis-Driven Review, 1900209*, 1–10. https://doi.org/10.1002/ejlt.201900209

Lethuaut, L., Métro, F., & Genot, C. (2002). *Effect of Droplet Size on Lipid Oxidation Rates of Ow Emulsion Stabilized By Protein, 79*(5), 425–430.

Lund, M. N., & Ray, C. A. (2017). *Control of Maillard Reactions in Foods: Strategies and Chemical Mechanisms.*. https://doi.org/10.1021/acs.jafc.7b00882

Manzocco, L., Calligaris, S., Anese, M., & Nicoli, M. C. (2016). Determination and Prediction of Shelf Life of Oils / Fats and Oil / Fat – Based Foods. Oxidative Stability and Shelf Life of Foods Containing Oils and Fats. Elsevier Inc. https://doi.org/10.1016/B978-1-63067-056-6.00002-1.

Martins, S. I. F. S., Jongen, W. M. F., & Van Boekel, M. A. J. S. (2001). *A review of Maillard reaction in food and implications to kinetic modelling, 11*, 364–373.

McClements, D. J., & Decker, E. A. (2000). Lipid Oxidation in Oil-in-Water Emulsions : Impact of Molecular Environment on Chemical. *Journal of Food Science, 65*(8), 1270–1282. Retrieved from http://lib3.dss.go.th/fulltext/Journal/Journal of food science/2000 vol 65/no.8/jfsv65n8p1270-1282ms20000241%5B1%5D.pdf.

Merkx, D. W. H., Swager, A., van Velzen, E. J. J., van Duynhoven, J. P. M., & Hennebelle, M. (2021). Quantitative and predictive modelling of lipid oxidation in mayonnaise. *Antioxidants, 10*(2), 1–14. https://doi.org/10.3390/antiox10020287

Miyashita, K. (2014). Highlight Article Paradox of omega - 3 PUFA oxidation, 1268–1279. https://doi.org/10.1002/ejlt.201400114.

Okubanjo, S. S., Ye, A., Wilde, P. J., Singh, H., & Loveday, S. M. (2021). Antioxidant performance in droplet-stabilized oil-in-water emulsions. *Lwt, 139*(November 2020), 110541. https://doi.org/10.1016/j.lwt.2020.110541.

Østdal, H., Davies, M. J., & Andersen, H. J. (2002). Reaction between protein radicals and other biomolecules. *Free Radical Biology and Medicine, 33*(2), 201–209. https://doi.org/10.1016/S0891-5849(02)00785-2

Pinchuk, I., & Lichtenberg, D. (2014). Analysis of the kinetics of lipid peroxidation in terms of characteristic time-points. *Chemistry and Physics of Lipids, 178*, 63–76. https://doi.org/10.1016/j.chemphyslip.2013.12.001

Pratt, D. A., Mills, J. H., & Porter, N. A. (2003). Theoretical calculations of carbon-oxygen bond dissociation enthalpies of peroxyl radicals formed in the autoxidation of lipids. *J Am Chem Soc, 125*, 5801–5810.

Riet, K. van 't, & Tramper, J. (1991). *Basic bioreactor design.* 99, Sectie Proceskunde, : CRC Press. Retrieved from https://edepot.wur.nl/478053.

Romsted, L. S., & Bravo-díaz, C. (2013). Current Opinion in Colloid & Interface Science Modeling chemical reactivity in emulsions. *Current Opinion in Colloid & Interface Science, 18*(1), 3–14. https://doi.org/10.1016/j.cocis.2012.11.001

Salminen, H., Heinonen, M., & Decker, E. A. (2010). Antioxidant effects of berry phenolics incorporated in oil-in-water emulsions with continuous phase β-Lactoglobulin. *JAOCS, Journal of the American Oil Chemists' Society, 87*(4), 419–428. https://doi.org/10.1007/s11746-009-1506-0

Schaich, K. M. (1992). Metals and lipid oxidation. *Contemporary issues. Lipids, 27*(3), 209–218.

Schaich, K. M. (2005). Lipid Oxidation: Theoretical Aspects. In Shahidi F (ed) (Ed.), *Bailey's Industrial Oil and Fat Products, Sixth Edition.* (p. pp 269–355). Hohn Wiley & Sons, Inc.

Schroën, C. G. P. H., Fretz, C. B., DeBruin, V. H., Berendsen, W., Moody, H. M., Roos, E. C., … Tramper, J. (2002). Modelling of the enzymatic kinetically controlled synthesis of cephalexin: Influence of diffusion limitation. *Biotechnology and Bioengineering, 80*(3). https://doi.org/10.1002/bit.10384

Schroën, C. G. P. H., Nierstrasz, V. A., Bosma, R., Kroon, P. J., Tjeerdsma, P. S., DeVroom, E., … Tramper, J. (2002). Integrated reactor concepts for the enzymatic kinetic synthesis of cephalexin. *Biotechnology and Bioengineering, 80*(2). https://doi.org/10.1002/bit.10348

Schroen, C. G. P. H., Nierstrasz, V. A., Moody, H. M., Hoogschagen, M. J., Kroon, P. J., Bosma, R., … Tramper, J. (2001). Modeling of the enzymatic kinetic synthesis of cephalexin - Influence of substrate concentration and temperature. *Biotechnology and Bioengineering, 73*(3), 171–178. https://doi.org/10.1002/bit.1049

Thomsen, M. K., Vedstesen, H., & Sikbsted, L. H. (1999). Quantification of radical formation in oil-imn-water emulsions by electron spin resonance spectroscopy. *Journal of Food Lipids, 6*(2), 149–158.

Venkateshwarlu, G., Let, M. B., Meyer, A. S., & Jacobsen, C. (2004). Modeling the Sensory Impact of Defined Combinations of Volatile Lipid Oxidation Products on Fishy and Metallic Off-Flavors. *Journal of Agricultural and Food Chemistry, 52*, 1635–1642. https://doi.org/10.1021/jf0351321

Viau, M., Genot, C., Ribourg, L., & Meynier, A. (2016). Amounts of the reactive aldehydes, malonaldehyde, 4-hydroxy-2-hexenal, and 4-hydroxy-2-nonenal in fresh and oxidized edible oils do not necessary reflect their peroxide and anisidine values. *European Journal of Lipid Science and Technology, 118*(3), 435–444. https://doi.org/10.1002/ejlt.201500103

Villeneuve, P., Bourlieu-Lacanal, C., Durand, E., Lecomte, J., McClements, D. J., & Decker, E. A. (2021). Lipid oxidation in emulsions and bulk oils: A review of the importance of micelles. *Critical Reviews in Food Science and Nutrition*, 1–41. https://doi.org/10.1080/10408398.2021.2006138

Westerterp, K. R., Van Swaaij, W. P. M., & Beenackers, A. A. C. M. (1987). *Chemical Reactor Design and Operation.* New York: John Wiley & Sons.

Yang, S., Verhoeff, A. A., Merkx, D. W. H., van Duynhoven, J. P. M., & Hohlbein, J. (2020). Quantitative spatiotemporal mapping of lipid and protein oxidation in mayonnaise. *Antioxidants, 9*(12), 1–13. https://doi.org/10.3390/antiox9121278